International Research Journal of Engineering and Technology (IRJET) e-ISSN: 2395-0056
Volume: 07 Issue: 08 | Aug 2020 www.irjet.net p-ISSN: 2395-0072

Performance Analysis of Unified Nonlinear Controller for Grid Connected PMSG based WECS

Ponrekha M[1], Sujatha Balaraman[2]

[1]PG Scholar, Government College of Technology, Coimbatore, Tamil nadu, India
[2]Associate Professor, Department of Electrical and Electronics Engineering, Government College of Technology, Coimbatore, Tamil nadu, India

---***---

Abstract - *In recent years, the need of renewable based power generation is growing exponentially due to high energy demand, depletion of existing fossil fuel deposits and carbon emission issue. Wind based power generation is gaining more interest among the existing renewable based power generation. The doubly-fed induction generator (DFIG) and permanent magnet synchronous generator (PMSG) are the most popular systems for wind energy conversion. The PMSG has attracted more attention due to its advantages of high-power density, high precision, high efficiency and reliability. In this research work, a single nonlinear multi input multi output (MIMO) controller based on feedback linearization method is designed for grid connected PMSG based wind energy conversion system (WECS). The simulation is done using MATLAB/Simulink and the performance of the controller is evaluated for different wind speeds under standalone and grid connected modes. The simulation results show that the developed control strategy provides a good performance.*

Key Words: **PMSG, wind energy conversion systems, stand-alone and grid-connected systems, nonlinear control, feedback linearization**

1. INTRODUCTION

Over the last twenty years, renewable energy sources are attracting more attention because of the price increase, restricted reserves and adverse environmental impact of fossil fuels. In the meantime, technological advancements, cost reduction and governmental incentives have made some renewable energy sources competitive in the market. Among them, wind energy is one among the quickest growing renewable energy sources.

Earlier wind energy has been used for milling grains, pumping water and sailing the seas. In the late nineteenth century, a 12 kW DC windmill generator was developed to generate electricity. It is, however, since the 1980s the technology has become sufficiently mature to supply electricity expeditiously and more reliably. Over the past twenty years, a spread of wind generation technologies is developed, that have improved the conversion potency and reduced the prices for wind energy production. Due to its limited applications, in addition to on-land installations, larger wind turbines are pushed to offshore locations to extract more energy and scale back their impact on land use and landscape.

Wind energy conversion systems (WECS) convert the kinetic energy associated with wind speed into electrical energy for feeding power to the grid. The power output from such wind energy conversion systems depend on the wind speed and the pitch angle of the turbine blades. Doubly fed induction generators (DFIGs) and Permanent magnet synchronous generators (PMSGs) are the most commonly used generators for WECS. PMSG has several advantages which make it very usable for WECS.

Installed capacity of wind power has been progressively growing over the last two decades. The installed capacity of global wind power has increased exponentially from approximately 6 GW in 2001 to 591 GW by 2018. In 2017, annual wind energy production grew 17%, reaching 4.4% of worldwide electric power usage, and providing 11.6% of the electricity in the European Union. This growth has been spurred by the continuous cost increase of classic energy sources, cost reduction of wind turbines, governmental incentive programs, and public demand for cleaner energy sources.

The wind turbines can operate as stand-alone units of small power capacity and supply power to villages, farms, and islands where access to the utility grid is remote or costly. Since the power generated from the wind is variable, other energy sources are normally required in stand-alone systems. A stand-alone wind energy conversion system operates with diesel generators, photovoltaic energy systems, or energy storage systems to form a more reliable distributed generation (DG) system. Stand-alone wind power constitutes only a small fraction of the total installed wind capacity in the world due to its limited applications. The majority of wind turbines operating in the field are grid-connected, and the power generated is directly injected to the grid. As most generators operate at a few hundred volts (typically 690 V), transformers are used to increase the generator voltage to tens of kilovolts, for example, 35 kV, for wind farm substations.

In this work, a single MIMO nonlinear controller is designed for grid connected PMSG based WECS and its performance is analysed in Matlab under varying wind velocities.

2. MATHEMATICAL MODELLING

The schematic diagram of the system is depicted in Fig. 1. It consists of a PMSG driven by a wind turbine, a generator side AC/DC converter, a grid-side DC/AC converter and MIMO controller. The wind turbine converts part of the kinetic energy of the wind into mechanical energy. This energy is converted into electrical energy via the generator. Since the generator output frequency is variable (depends on the wind conditions), a back-to-back converter is used to synchronized its output with the grid frequency [1].

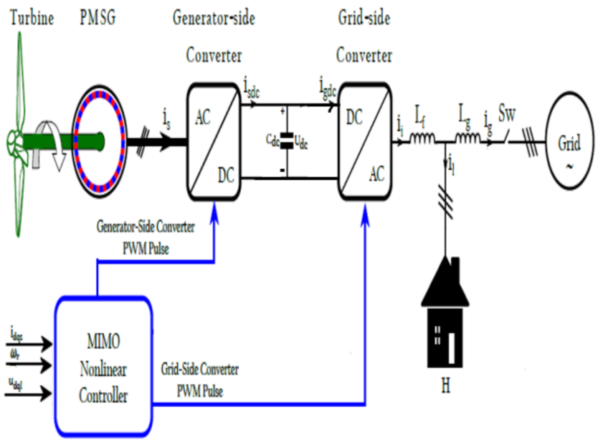

Fig -1: Schematic diagram of PMSG based WECS

2.1 Modelling of Wind Turbine

The wind turbine retrieves only a fraction of the wind's kinetic power. This power is determined by the area swept by the blades, S_ω ($S_\omega = \pi R^2$), the wind speed, v_ω ,the air density, ρ, and the power coefficient, C_p, which characterizes each turbine. Hence, the generated mechanical power, can be expressed as follows:

$$P_m = \frac{1}{2}\pi\rho C_p(\lambda,\beta)R^2 {v_\omega}^3 \tag{1}$$

$$\lambda = \frac{\omega_m R}{v_\omega} \tag{2}$$

where R is the radius of the turbine, C_p is the power coefficient which is a function of λ, the tip speed ratio and β, the pitch angle. ω_m is the turbine angular speed. Neglecting the friction forces, the dynamic equation of the wind turbine is given by

$$\frac{d\omega_m}{dt} = \frac{P}{J}(T_m - T_e) \tag{3}$$

where $\omega_m$is the rotating speed of the blade, P, the number of pole pairs, J, the moment of inertia of the generator, T_m, the torque developed by the turbine and T_e, the torque due to load which in this case is the generator electromagnetic torque.

2.2 Modelling of PMSG

The PMSG converts the mechanical energy obtained from the wind turbine to electrical energy. In order to simplify its analysis, the three-phase PMSG is modelled in the dq reference frame. It is given by

$$u_{ds} = R_s i_{ds} + L_d \frac{di_{ds}}{dt} - \omega_r L_q i_{qs} \tag{4}$$

$$u_{qs} = R_s i_{qs} + L_q \frac{di_{qs}}{dt} + \omega_r L_q i_{ds} + \omega_r \lambda_r \tag{5}$$

$$T_e = \frac{3P}{2}\left[\lambda_r i_{qs} - \left(L_d - L_q\right) i_{ds} i_{qs}\right] \tag{6}$$

where u_{ds}, u_{qs} and i_{ds}, i_{qs} are the generator stator dq-axis voltages (V) and currents (A), respectively; Rs is the stator winding resistance (Ω); L_d and L_q are the stator dq-axis self-inductances (H); ω_r is the rotor electrical angular speed (rad/s); and λ_r is the rotor flux (Wb) generated by the permanent magnets. Non-salient (or round) rotor PMSG is considered in this study, the d- and q-axis magnetizing inductances are therefore equal ($L_d = L_q$).

2.3 Modelling of Back-to-Back Converter

The back-to-back (B2B) converter consists of two identical voltage source converters (VSC) and a capacitor which is connected in between them. The generator-side VSC converts the three-phase generator AC output signal into DC voltage, whereas the grid-side VSC converts the DC voltage into the load input three-phase AC voltage. The load voltage will be controlled through the grid-side VSC. Its dq reference frame output voltage model is given by

$$u_{di} = L_f \frac{di_{di}}{dt} - \omega_g L_f i_{qi} + u_{dl} \tag{7}$$

$$u_{qi} = L_f \frac{di_{qi}}{dt} + \omega_g L_f i_{di} + u_{ql} \tag{8}$$

where u_{di}, u_{qi} and i_{di}, i_{qi} are the grid-side converter output dq-axis voltages (V) and currents (A), respectively; u_{dl} and u_{ql} are the load dq-axis voltage (V); L_f and ω_g are the grid side filter inductance (H) and the grid electrical angular speed (rad/s), respectively.

2.4 Modelling of Grid side circuit

The grid-side circuit is composed of a RL load, a filter, L_f, the line inductance, L_g, and the grid when the system operates in the grid-connected mode. For the sake of simplicity, the transformer leakage inductance is included in L_g. One of the advantages of the proposed control system is that the voltage of the load is constantly controlled in grid-connected mode and stand-alone mode. It is therefore not necessary to use a capacitor in the output filter of the converter.

The main idea behind this modelling approach is to represent the grid and the load by an equivalent Thevenin model. This model will be connected in series with L_f at A as illustrated in Fig. 2. If $Z_l = R_l + j\omega_g L_l$ denotes the load impedance and $u_g = u_{dg} + ju_{qg}$ represents the grid voltage, then the Thevenin voltage and impedance in the grid-connected mode are given respectively by

$$E_{th} = \frac{(R_l+j\omega_g L_l)(u_{dg}+ju_{qg})}{R_l+j\omega_g(L_l+L_g)} \quad (9)$$

$$Z_{th} = \frac{j\omega_g L_g(R_l+j\omega_g L_l)}{R_l+j\omega_g(L_l+L_g)} \quad (10)$$

Note that R_l and L_l are obtained from the active and reactive power supplied to the load as follows

$$R_l = \frac{\sqrt{3}\, u_{ll}^2 P_l}{P_l^2+Q_l^2} \text{ and } L_l = \frac{\sqrt{3}\, u_{ll}^2 Q_l}{P_l^2+Q_l^2} \quad (11)$$

where u_{ll} is the load line-to-line RMS voltage. P_l and Q_l are the load active and reactive power of the system, respectively. They can be obtained from the load current and voltage

$$P_l = \frac{3}{2}(u_{dl}i_{dl} + u_{ql}i_{ql}) \quad (12)$$

$$Q_l = \frac{3}{2}(u_{ql}i_{dl} - u_{dl}i_{ql}) \quad (13)$$

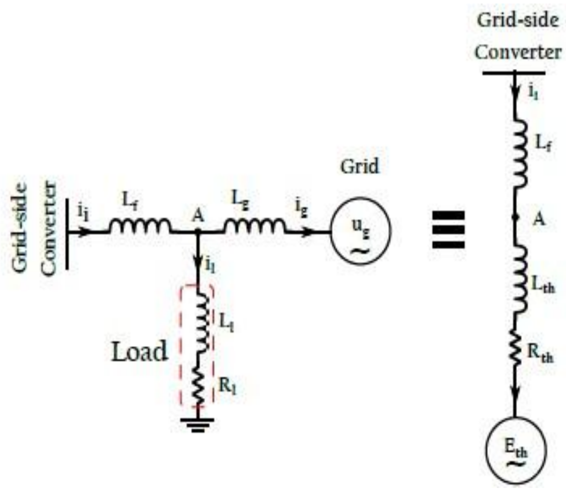

Fig -2: Grid-side circuit and the respective Thevenin equivalent circuit

When the grid is not available (in the stand-alone mode), the Thevenin voltage and impedance are respectively given by

$$E_{th} = 0 \quad \text{and} \quad Z_{th} = Z_l \quad (14)$$

The grid-side circuit is assumed in a quasi-static mode, therefore, the following relationships are valid

$$u_{dl} = R_{th}i_{di} - \omega_g L_{th}i_{qi} + E_{thd} \quad (15)$$

$$u_{ql} = R_{th}i_{qi} + \omega_g L_{th}i_{di} + E_{thq} \quad (16)$$

where R_{th} and $\omega_g L_{th}$ are real and imaginary parts of the Thevenin impedance, respectively ($Z_{th} = R_{th} + j\omega_g L_{th}$).

3. FEEDBACK LINEARIZATION

Feedback linearization is a method for nonlinear control design which has attracted a great deal of research interest in recent years. The central idea of this method is to algebraically transform the nonlinear dynamics of a system into a (fully or partly) linear one, so that linear control techniques can be applied[6].

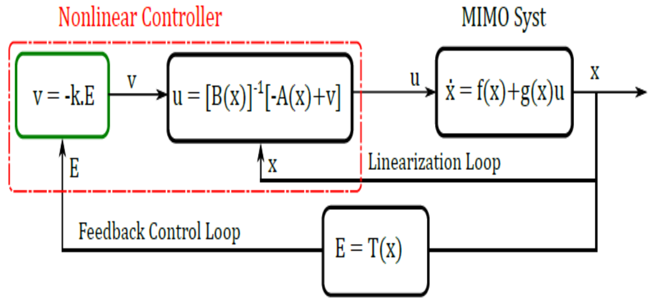

Fig -3: MIMO controller structure

The controller is designed using the input-output feedback linearization method. The MIMO controller will calculate and generate the appropriate control signals for each converter.

The control objectives are to:

1) keep the wind turbine operating at its maximum power by controlling ω_r

2) achieve a linear relationship between the stator current and the electromagnetic torque by controlling the stator d-axis current, i_{ds}

3) meet load voltage requirement by controlling both load d-axis and q-axis voltages, u_{dl} and u_{ql} respectively.

In this study, $i_{ds}, i_{qs}, \omega_r, i_{di}, i_{qi}$ are taken as state variables, $u_{ds}, u_{qs}, u_{di}, u_{qi}$ are taken as input variables and $\tilde{i}_{ds}, \tilde{\omega}_r, \tilde{u}_{dl}, \tilde{u}_{ql}$ are considered as output variables.

$$\bar{x} = [i_{ds}, i_{qs}, \omega_r, i_{di}, i_{qi}]^T \quad (17)$$

$$\bar{u} = [u_{ds}, u_{qs}, u_{di}, u_{qi}]^T \quad (18)$$

$$\bar{y} = [\tilde{i}_{ds}, \tilde{\omega}_r, \tilde{u}_{dl}, \tilde{u}_{ql},]^T \quad (19)$$

where,

$$\tilde{i}_{ds} = \int (i_{ds} - i_{ds}^*)d\delta \quad (20)$$

$$\tilde{\omega}_r = \int (\omega_r - \omega_r^*)d\delta \quad (21)$$

$$\tilde{u}_{dl} = \int (u_{dl} - u_{dl}^*)d\delta \quad (22)$$

$$\tilde{u}_{ql} = \int (u_{ql} - u_{ql}^*)d\delta \quad (23)$$

To ensure zero steady state error and to increase the robustness of the controller when the system structure changes, integral actions are added into the control-loop. This happens, for instance, when the system switches from the stand-alone mode to the grid connected mode. The input output feedback linearization control design method is used to linearize and decouple this nonlinear model. Each output is differentiated therefore until at least one input appears. However, it can be noted that each controlled variable has been differentiated twice, before a control input emerges, except for $\tilde{\omega}_r$ which has been differentiated three times.

The state equation is

$$\begin{bmatrix} \ddot{i}_{ds} \\ \dddot{\omega}_r \\ \ddot{u}_{dl} \\ \ddot{u}_{ql} \end{bmatrix} = \begin{bmatrix} A_1 \\ A_2 \\ A_3 \\ A_4 \end{bmatrix} + \begin{bmatrix} \frac{1}{L_d} & 0 & 0 & 0 \\ 0 & \frac{3P^2\lambda_r}{2JL_q} & 0 & 0 \\ 0 & 0 & \frac{R_{th}}{L_f} & -\frac{\omega_g L_{th}}{L_f} \\ 0 & 0 & \frac{\omega_g L_{th}}{L_f} & \frac{R_{th}}{L_f} \end{bmatrix} \begin{bmatrix} u_{ds} \\ u_{qs} \\ u_{di} \\ u_{qi} \end{bmatrix} \tag{4.8}$$

Where,

$$A_1 = -\frac{R_s}{L_d} i_{ds} + \frac{L_q}{L_d}\omega_r i_{qs}$$

$$A_2 = -\frac{3P^2}{2JL_q}\lambda_r\left(-L_d\omega_r i_{ds} - R_s i_{qs} - \lambda_r\omega_r\right) - \frac{2K_{opt}\omega_r}{PJ^2}\left(\frac{3P^2\lambda_r}{2} i_{qs} - \frac{K_{opt}\omega_r^2}{P}\right)$$

$$A_3 = R_{th}\left(\omega_g i_{qi} - \frac{u_{dl}}{L_f}\right) - \omega_g L_{th}\left(-\omega_g i_{di} - \frac{u_{ql}}{L_f}\right) + \dot{E}_{thd}$$

$$A_4 = R_{th}\left(-\omega_g i_{di} - \frac{u_{ql}}{L_f}\right) + \omega_g L_{th}\left(\omega_g i_{qi} - \frac{u_{dl}}{L_f}\right) + \dot{E}_{thq}$$

The control law has the following form

$$\bar{u} = [B(\bar{x})]^{-1}[-A(\bar{x}) + \bar{v}] \tag{4.9}$$

By choosing u as in Eqn. (23), the nonlinearities in Eqn. (22) are cancelled and the following linear relationship between the new outputs $y_d(\bar{x})$ and the new inputs, $\bar{v}$, is obtained.

$$y_d(\bar{x}) = \bar{v} \tag{4.10}$$

Where,

$$y_d(\bar{x}) = [\ddot{i}_{ds}, \dddot{\omega}_r, \ddot{u}_{dl}, \ddot{u}_{ql}]^T$$

$$\bar{v} = [v1, v2, v3, v4]^T$$

Note that the total relative degree (r = 7) is equal to the order of the system n (n = 7). Therefore, the linearization is complete and there is no internal dynamics. A state feedback controller is used. It has the following equation:

$$v_p = -k_{pq} e_p \tag{4.11}$$

where k_{pq} ($p \in \{1,2,3,4,5,6\}$ and $q \in \{1,2,3\}$) is the feedback gain matrix and e_p represents the errors between the outputs variables ($\tilde{i}_{ds}$, $\tilde{\omega}_r$, $\tilde{u}_{dl}$, and $\tilde{u}_{dql}$) and the reference signals. These references are equal to zero. Therefore, the expressions of v_p ($p \in \{1,2,3,4,5,6\}$) are as follows:

$$v_1 = -k_{11}\tilde{i}_{ds} - k_{12}\dot{\tilde{i}}_{ds}$$

$$v_2 = -k_{21}\tilde{\omega}_r - k_{22}\dot{\tilde{\omega}}_r - k_{23}\ddot{\tilde{\omega}}_r$$

$$v_3 = -k_{31}\tilde{u}_{dl} - k_{32}\dot{\tilde{u}}_{dl}$$

$$v_4 = -k_{41}\tilde{u}_{ql} - k_{42}\dot{\tilde{u}}_{ql} \tag{4.12}$$

Where, k_{ij}, is the feedback gain matrix [1]. The reference signals, such as $i_{ds}{}^*$, $\omega_r{}^*$, $u_{dl}{}^*$, $u_{ql}{}^*$ are chosen considering the following points.

1) $i_{ds}{}^*$ is set to zero to realize the zero d-Axis current (ZDC) control scheme. This control scheme is employed to achieve a linear relationship between the stator current and the electromagnetic torque.

2) $\omega_r{}^*$ is generated by the MPPT with optimal tip speed ratio.

3) $u_{dl}{}^*$ is aligned with the grid voltage vector to achieve voltage-oriented control (VOC). Therefore, $u_{dl}{}^*$ is equal to the grid voltage magnitude. Hence $u_{ql}{}^*$ is equal to zero.

The synchronization to the grid is done by using a PLL (Phase-locked Loop). Therefore, in the grid connected mode, the grid frequency (ω_g) which is used in the dq-abc coordinate transformation is generated by the PLL.

4. RESULTS AND DISCUSSION

The simulation is carried out using Matlab. The system consider for simulation comprises 2.45 MW variable speed non-salient pole PMSG generator is employed and the respective parameters are shown in Table -1 [5].

Case 1: System under standalone mode

The Simulink Model of PMSG based WECS under standalone mode is shown in fig-3. The inputs to the turbine are wind speed, pitch angle and generator speed. The output torque of the wind turbine is given to the PMSG as input. To analyze the behavior of PMSG under varying wind speed, three wind speeds are considered. For simulation, initial wind speed is taken as 12m/s and it falls to 8m/s at 1.5 time units and then reduces to 5m/s at 2.5-time units. The torque output of wind turbine is shown in fig-4. The torque is found to be negative since the Permanent Magnet Synchronous machine act as Generator.

The rotor speed of PMSG varies according to wind speed is shown in fig-5. When the wind speed is high, rotor speed is also high. As the wind speed reduces, rotor speed also reduces. The output voltage and current of PMSG for varying speed are measured. It shows that the generated voltage and current are high when the wind speed is high and vice versa. The simulated waveforms of the rotor speed ω_r and generator output power P_m show that the PMSG output power depends on wind speed.

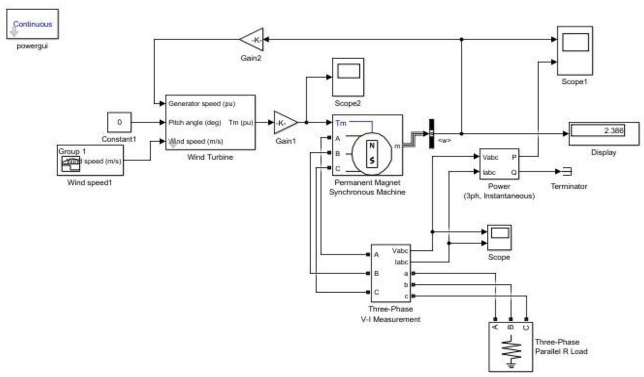

Fig -3: Simulink Model of PMSG based WECS under standalone mode

Table -1: Parameters of the system

Parameter	Rated Value
P_m	$2.5\ MW$
ω_m	$4.3\ rad/s$
λ_r	$28\ wb$
P	8
J	$4000\ kgm^2$
R_s	$24.21\ m\Omega$
L_{ds}, L_{qs}	$9.81 mH$
v_m	$15\ m/s$
u_g	$4kV$
u_{dc}	$8\ kV$
C_{dc}	$1667 \mu F$
L_f	$16.884\ mH$
L_g	$1.6884\ \mu H$
u_{ll}	$4kV$

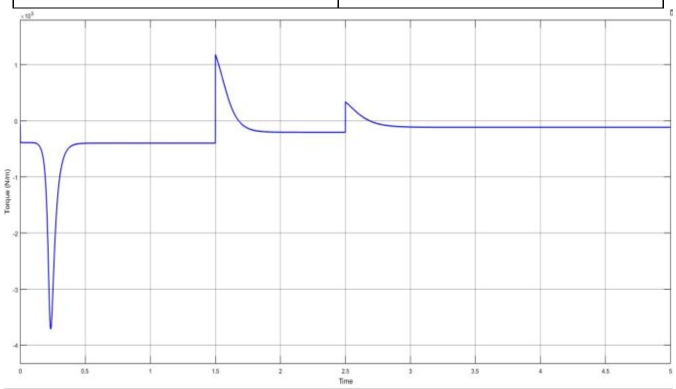

Fig -4: Torque output of Wind turbine

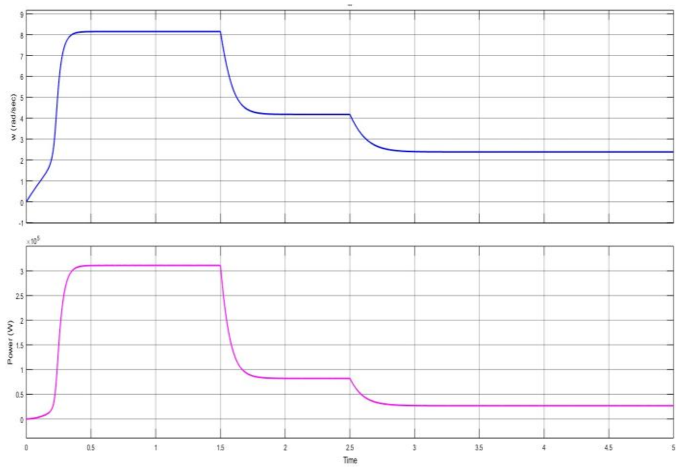

Fig -5: Rotor speed and output power of PMSG

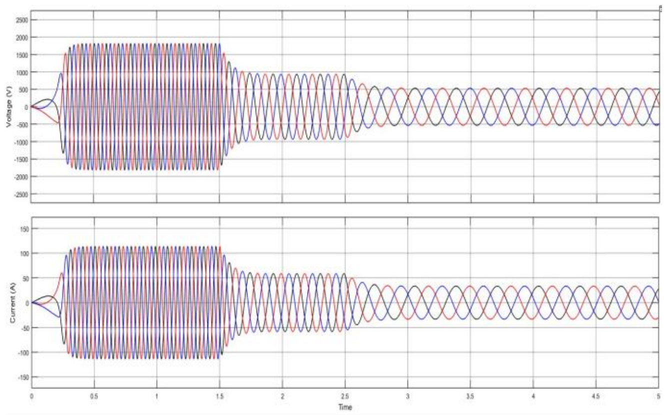

Fig -6: Output Voltage and current waveforms of PMSG

Case 2: Grid connected system

The Simulink Model of PMSG based WECS under grid connected mode is shown in fig-6. The inputs to the turbine are wind speed, pitch angle and generator speed. The output torque of the wind turbine is given to the PMSG as input. The output of PMSG is given to the back to back converter to synchronize the variable frequency of PMSG with the grid frequency. The load is connected between back to back converter and the grid.

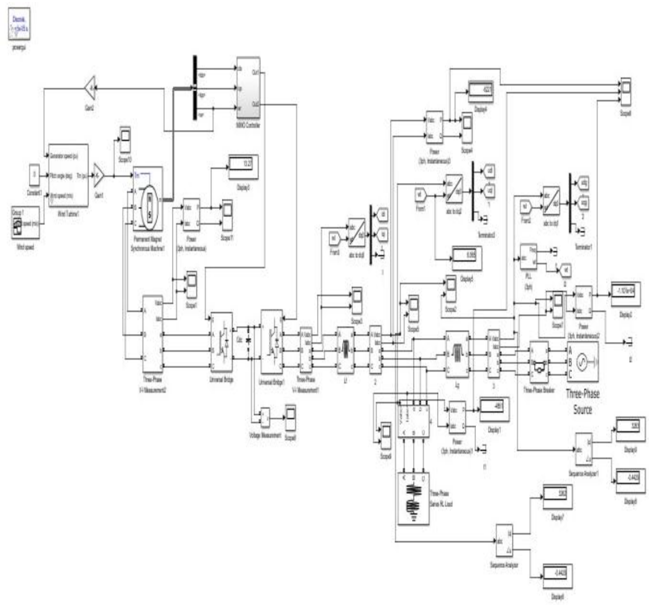

Fig -7: Simulink Model of Grid connected PMSG based WECS

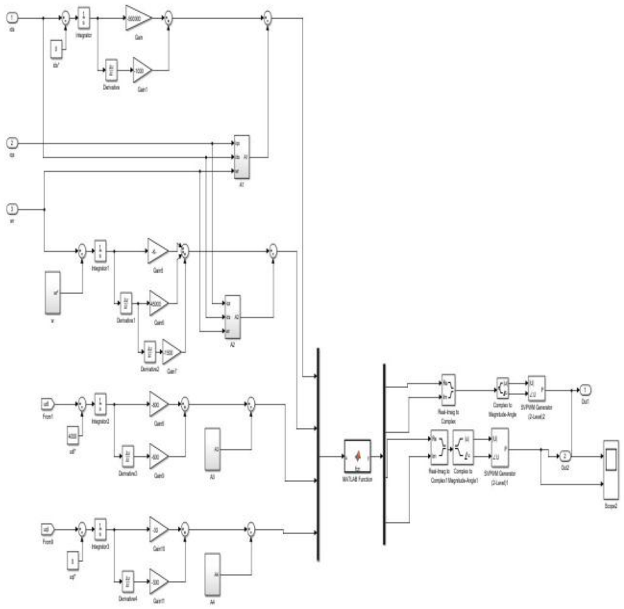

Fig -8: Simulink Model of MIMO Controller for Grid connected PMSG based WECS

The Simulink Model of MIMO Controller for grid connected PMSG based WECS is shown in fig-8. The synchronization to the grid is done by using a PLL (Phase-locked Loop). Therefore, in the grid connected mode, the grid frequency which is used in the dq-abc coordinate transformation is generated by the PLL. The Controller is designed based on the equations (4.8) to (4.12). The controller gains are considered from [1].

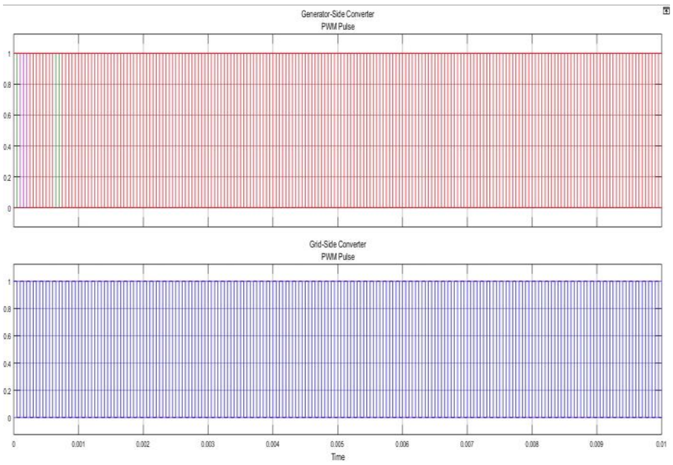

Fig -9: Generated PWM pulses for Generator and Grid side converter

The reference rotor speed is calculated by using MPPT with optimal tip speed ratio. The measured wind speed v_ω is used to produce the generator speed reference ω_r^* according to the optimal tip speed ratio $\lambda_{opt} = 8.1$. The MIMO controller is able to calculate and generate the required PWM pulses for Generator and Grid side converters. The output pulses are shown in fig-9. The control pulses are generated by controlling the output variables, rotor speed, stator direct axis current and dq components of load voltage.

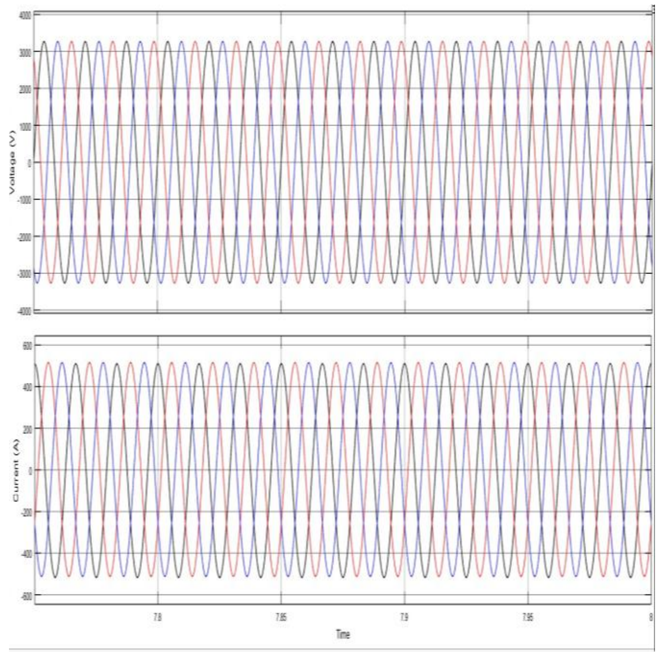

Fig -10: Voltage and Current waveforms at the point of common coupling (PCC)

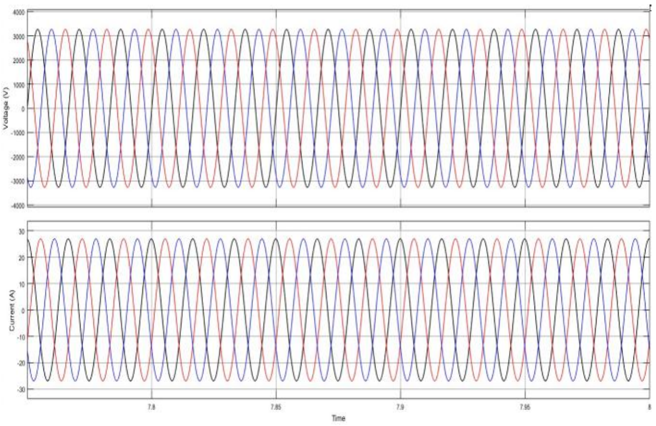

Fig -11: Voltage and Current waveforms of three phase balanced load

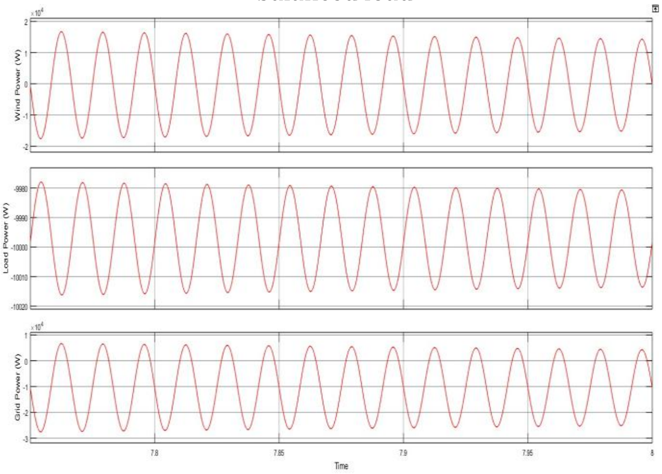

Fig -12: Real Power - PMSG, Load and Grid

The real power of Grid, PMSG and power drawn by load at a wind speed of 15m/s are shown in fig-12. It is revealed that when the wind speed is high, power generated by PMSG is also more and it contributes majority of the power to the load and so the grid contributes only required minimum power in order to maintain the power balance.

5. CONCLUSION

In this research work, ~~a~~ unified nonlinear controller is designed for grid connected PMSG based WECS. It differs from the conventional methods found in literature, where a separate controller, PID based for each mode of operation was employed. MIMO feedback linearization control technique is adopted in this study. Integrators are added into the control-loop to ensure zero steady state errors when the operating point changes. When compared to conventional methods which employs greater number of PI controllers, MIMO controller-based control strategy is cost effective. The simulation is carried out using Matlab and the performance of the MIMO controller has been tested for varying wind speeds. The simulation results show that the proposed control strategy provides a good performance than the conventional one.

REFERENCES

[1] Boubacar Housseini, Aime Francis Okou, Rachid Beguenane, 2017, "Robust Nonlinear Controller Design for On-grid/Off-grid Wind Energy Battery-Storage System", IEEE Transactions on Smart Grid, vol. 9, no. 5, pp. 5588–5598.

[2] Ki-Hong Kim, Yoon-Cheul Jeung, Dong-Choon Lee , 2012, "Lvrt scheme of pmsg wind power systems based on feedback linearization", IEEE Transactions on Power Electronics, vol. 27, no. 5, pp. 2376–2384.

[3] José Matas, Miguel Castilla, Josep M. Guerrero, Luis García de Vicuña and Jaume Miret, 2008, "Feedback Linearization Of Direct-Drive Synchronous Wind-Turbines Via a Sliding Mode Approach", IEEE Transactions on Power Electronics, vol. 23, no. 3, pp. 1093–1103.

[4] R. Teodorescu and F. Blaabjerg, 2004, "Flexible control of sall wind turbines with grid failure detection operating in stand-alone and grid-connected mode", IEEE Transactions on Power Electronics, vol. 19, no. 5, pp. 1323–1332.

[5] B. Wu, Y. Lang, N. Zargari, and S. Kouro, 2011, "Power conversion and control of wind energy systems". John Wiley & Sons, vol. 77.

[6] B. Housseini, F. A. Okou, and R. Beguenane, 2015, "A unified nonlinear controller design for on-grid/off-grid wind energy battery-storage system," in Industrial Electronics Society, IECON 2015-41st Annual Conf. of the IEEE. IEEE, pp. 005 273–005 278.

[7] J.-J. E. Slotine, W. Li et al., 1991, "Applied nonlinear control". Prentice-Hall Englewood Cliffs, NJ, vol. 199, no. 1.

[8] D. Gaonkar, R. Patel, and G. Pillai, 2006, "Dynamic model of microturbine generation system for grid connected/islanding operation," in Industrial Technology, ICIT 2006. IEEE Inter. Conf. on. IEEE, pp. 305–310.

[9] F. Gao and M. R. Iravani, 2008, "A control strategy for a distributed generation unit in grid-connected and autonomous modes of operation," IEEE Trans. on power delivery, vol. 23, no. 2, pp. 850–859.

[10] M. Fatu, F. Blaabjerg, and I. Boldea, 2014, "Grid to standalone transition motion-sensorless dual-inverter control of pmsg with asymmetrical grid voltage sags and harmonics filtering," IEEE Transactions on Power Electronics, vol. 29, no. 7, pp. 3463–3472.

[11] M. Morawiec, "The adaptive backstepping control of permanent magnet synchronous motor supplied by current source inverter," Industrial Informatics, IEEE Transactions on, vol. 9, no. 2, pp. 1047–1055, 2013.

[12] M. N. Arafat, S. Palle, Y. Sozer, and I. Husain, 2012 "Transition control strategy between standalone and grid-connected operations of voltage source inverters," Industry Applications, IEEE Transactions on, vol. 48, no. 5, pp. 1516–1525.

[13] Z. Yao, L. Xiao, and Y. Yan, 2010, "Seamless transfer of single-phase gridinteractive inverters between grid-connected and stand-alone modes," IEEE Transactions on Power Electronics, vol. 25, no. 6, pp. 1597–1603.